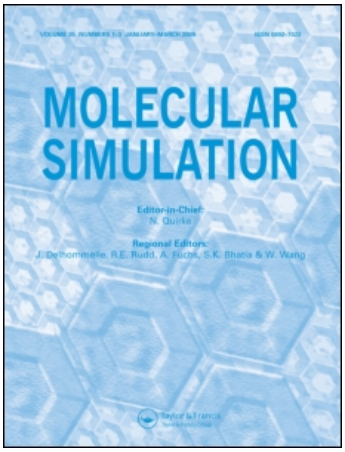

Molecular Simulation
Publication details, including instructions for authors and subscription information:
http://www.informaworld.com/smpp/title~content=t713644482

Explicit-solvent molecular dynamics simulations of a DNA tetradecanucleotide duplex: lattice-sum versus reaction-field electrostatics

Vincent Kräutler[a]; Philippe H. Hünenberger[a]
[a] Laboratory of Physical Chemistry, ETH Zürich, Zürich, Switzerland

To cite this Article Kräutler, Vincent and Hünenberger, Philippe H.(2008) 'Explicit-solvent molecular dynamics simulations of a DNA tetradecanucleotide duplex: lattice-sum versus reaction-field electrostatics', Molecular Simulation, 34: 5, 491 — 499
To link to this Article: DOI: 10.1080/08927020701783566
URL: http://dx.doi.org/10.1080/08927020701783566

Molecular Simulation
Vol. 34, No. 5, April 2008, 491–499

Taylor & Francis
Taylor & Francis Group

Explicit-solvent molecular dynamics simulations of a DNA tetradecanucleotide duplex: lattice-sum versus reaction-field electrostatics

Vincent Kräutler and Philippe H. Hünenberger*

Laboratory of Physical Chemistry, ETH Zürich, CH-8093 Zürich, Switzerland

(Received 9 October 2007; final version received 15 October 2007)

Five long-timescale (10 ns) explicit-solvent molecular dynamics simulations of a DNA tetradecanucleotide dimer are performed using the GROMOS 45A4 force field and the simple-point-charge water model, in order to investigate the effect of the treatment of long-range electrostatic interactions as well as of the box shape and size on the structure and dynamics of the molecule (starting from an idealised B-DNA conformation). Long-range electrostatic interactions are handled using either a lattice-sum (LS) method (particle–particle–particle–mesh; one simulation performed within a cubic box) or a cutoff-based reaction-field (RF) method (four simulations, with long-range cutoff distances of 1.4 or 2.0 nm and performed within cubic or truncated octahedral periodic boxes). The overall double-helical structure, including Watson–Crick (WC) base-pairing, is well conserved in the simulation employing the LS scheme. In contrast, the WC base-pairing is nearly completely disrupted in the four simulations employing the RF scheme. These four simulations result in highly distorted compact (cutoff distance of 1.4 nm) or extended (cutoff distance of 2 nm) structures, irrespective of the shape and size of the computational box. These differences observed between the two schemes seem correlated with large differences in the radial distribution function between charged entities (backbone phosphate groups and sodium counterions) within the system.

Keywords: DNA oligonucleotide; computer simulation; molecular dynamics; electrostatic interactions; GROMOS force field

1. Introduction

The last two decades have witnessed a significant increase in the number of publications reporting atomistic (explicit-solvent) molecular dynamics (MD) simulations of nucleic acids in aqueous solution [1–8]. However, in spite of significant methodological advances, nucleic acids remain very challenging systems for computational modelling, because their polyelectrolyte nature (as well as the possible simultaneous inclusion of many counterions) implies the need for a particularly accurate treatment of (long-range) electrostatic interactions [9].

In order to avoid surface effects, the vast majority of explicit-solvent molecular simulations are carried out under periodic boundary conditions (PBC). In this case, the two (currently) most popular approximations used to handle long-range electrostatics are the lattice-sum (LS) and reaction-field (RF) methods.

The LS methods (applied under PBC) rely on accepting the exact periodicity of electrostatic interactions as an intrinsic property of the simulated system. In this case, electrostatic interactions can be handled exactly (within the limit of numerical accuracy) using the Ewald [10] or related particle–mesh (P^3M [11,12] or PME [13,14]) methods. Accepting electrostatic periodicity is certainly quite reasonable for performing simulations of crystals. However, solutions are inherently non-periodic systems, and the use of LS methods in this context can be summarised as providing exact electrostatic interactions for an approximate (i.e. artificially periodic) representation of the system [15,16]. Recent studies aimed at quantifying the effects of artificial periodicity in biomolecular simulations have often led to contradictory results [17–30], probably in large part because the nature and magnitude of possible artefacts are very sensitive to the simulated system and simulation conditions (e.g. solute net charge and dipole moment, size of the solute cavity relative to that of the computational box, presence and concentration of counterions, dielectric permittivity of the solvent and system properties monitored).

The RF method (applied under PBC) relies on truncating electrostatic interactions to a finite range (cutoff distance), typically smaller than half the smallest dimension of the computational box, and accounting for the mean effect of the omitted electrostatic interactions beyond this distance by modelling the medium outside the cutoff sphere of each particle as a homogeneous

*Corresponding author. Email: phil@igc.phys.chem.ethz.ch

ISSN 0892-7022 print/ISSN 1029-0435 online

DOI: 10.1080/08927020701783566
http://www.informaworld.com

dielectric medium of permittivity equal to that of the solvent [31–34]. This approximation (given a large-enough cutoff distance) is certainly reasonable for the simulation of pure (dipolar) liquids. However, biomolecular solutions are typically: (i) dielectrically heterogeneous (i.e. the medium outside the cutoff sphere of a particle is generally not entirely bulk solvent); and (ii) rich in entities (solute functional groups, counterions) bearing net charges (i.e. for which the RF formalism is not strictly applicable). Thus, the use of the RF method in this context can by summarised as providing approximate electrostatic interactions for a more realistic (i.e. quasi-nonperiodic) representation of the system [15]. In principle, the RF method should benefit from the use of large cutoff distances. A common time-saving technique for increasing the effective cutoff radius with a limited computational overhead is the twin-range (TW) method, where interactions up to a short-range cutoff distance are evaluated every simulation timestep, while interactions between the short-range and long-range cutoff distances are evaluated less frequently and assumed constant between two evaluations [35].

After numerous unsuccessful attempts to perform explicit-solvent molecular simulations of nucleic acids using straight-cutoff truncation [36,37], it was realised that the use of LS methods instead permitted to obtain trajectories of DNA oligonucleotide dimers with a stable double-helical (native) conformation on timescales up to 400 ns [5]. The RF method was also applied with some success, but only on much shorter timescales of at most 2 ns [38–42]. In addition, significant base-pair fraying at the strand termini (expected to occur only on a millisecond timescale [43,44]) was found in all of these RF simulations. A likely cause for this is the use of group-based cutoff schemes which, for groups bearing net charges, are known to cause significant heating in the cutoff region [45]. Simulations of stable (up to 5 ns) DNA duplexes using atom-based force-shifting methods [46] have also been reported [37,47,48].

Unfortunately, it is difficult to rigorously and unambiguously compare the effect of different treatments of electrostatic interactions in simulations of nucleic acids, because the three main sources of errors affecting these simulations in practice are difficult to disentangle: (i) limited accuracy of the employed force-field (functional form and parameters, i.e. the native structure may be intrinsically unstable within a given force-field, even with a hypothetically exact treatment of the electrostatic interactions); (ii) approximate treatment of electrostatic interactions (i.e. the native structure may be artificially stabilised or destabilised by inaccurate electrostatics, independent of its inherent stability within the force-field employed); and (iii) insufficient sampling (i.e. the native structure may appear stable on a given timescale, even if it is intrinsically unstable within the chosen force-field representation and treatment of electrostatics; furthermore, the timescale on which this apparent stability is maintained may depend on the two latter choices).

In order to provide more insight into the specific role of electrostatics, we report here five long-timescale (10 ns) explicit-solvent simulations of a DNA tetradecanucleotide dimer in water using the GROMOS 45A4 force-field [49,50] together with different treatments of electrostatic interactions (LS or RF), cutoff distances (RF only) and computational box shape and size (RF only).

2. Computational details

Five explicit-solvent MD simulations of 10 ns duration were performed in order to examine the influence of the electrostatics scheme (TW/RF or LS), of the cutoff distance (TW/RF only) and of the box geometry and size (cubic, CU, or truncated octahedral, TO, box; the latter for TW/RF only) on the structure and dynamics of a DNA tetradecanucleotide dimer with sequence [51] 5′-(GCATTCTGAGTCAG)-3′:5′-(CTGACTCAGAATGC)-3′ in water.

The simulations were carried out using the GROMOS96 [35,52] and GROMOS05 [53] packages of programs together with the GROMOS 45A4 force field [50] including a recently refined parameter set for DNA [49], and the simple-point-charge (SPC) water model [54]. The equations of motion were integrated using the leapfrog scheme [55] with a timestep of 2 fs. All bond lengths were constrained by application of the SHAKE algorithm [56] with a relative geometric tolerance of 10^{-4}. Solute and solvent degrees of freedom were independently coupled to a heat bath at 300 K with a relaxation time of 0.1 ps [57]. The box dimensions were isotropically coupled to a pressure bath [57] at 1 atm, with a relaxation time of 0.5 ps and an isothermal compressibility of $45.75 \times 10^{-5}\,\mathrm{kJ^{-1}\,mol\,nm^3}$. The centre of mass motion was removed every 2 ps. Trajectory frames were written to file every 1 ps for later analysis.

The nonbonded interactions were handled in either of two ways. In the TW/RF scheme (four simulations), a TW cutoff scheme [35] was employed for both electrostatic and Lennard-Jones interactions, with a short-range cutoff radius of 0.8 nm, a long-range cutoff radius of either 1.4 or 2 nm, and a frequency of five timesteps for the update of the short-range pairlist and intermediate-range interactions. Simultaneously, a RF correction [34] was applied to account for the mean effect of electrostatic interactions due to the solvent beyond the long-range cutoff radius, using a relative dielectric permittivity of 60 as appropriate for the SPC water model [58]. In the LS scheme (one simulation),

electrostatic interactions were handled using the particle–particle–particle–mesh (P^3M) method [11,12], using a real-space cutoff distance of 0.6 nm (pairlist updated every five timesteps), a spherical-hat charge-shaping function [59], an assignment function of order 3, a finite-difference interpolation of order 3, a mesh of $64 \times 64 \times 64$ points and tinfoil boundary condition. In this scheme, the Lennard-Jones interactions were truncated at a distance of 1.4 nm (pairlist updated every five steps).

The simulated systems were prepared in either of two ways, starting from a model double-helical structure of the tetradecanucleotide dimer corresponding to an idealised B-DNA conformation. In the CU case, the solute was placed at the centre of a (periodic) cubic box of edge length 6.6 nm, containing 9086 water molecules. In the TO case, the solute was placed at the centre of a (periodic) truncated octahedral box based on a cube of edge length 7.7 nm, containing 6953 water molecules. A total of 26 randomly selected water molecules were then replaced by an equal number of sodium ions, so as to neutralise the system. The resulting systems were relaxed as described elsewhere [60,61], using steepest-descent energy minimisation, followed by 50 ps equilibration with positional restraints on the nucleotide atoms, the corresponding harmonic force constant being gradually reduced from 20 to 4 kJ mol^{-1} nm^{-2}. This equilibration was followed by 10 ns production simulations for the five combinations of electrostatic scheme, cutoff distance and box geometry considered in the present study. To simplify the discussion, each of these simulations is associated with a unique code as summarised in Table 1.

The simulations were analyzed in terms of atom-positional root-mean-square-deviation (RMSD) from the initial (idealised) B-DNA structure, solute radius of gyration (R_{gyr}), intra-solute Watson–Crick (WC) hydrogen bonds (H—bonds) and base-pairing [62], and radial distribution functions (RDF) between charged entities.

The RMSD was calculated along each trajectory at 10 ps intervals, based on all atoms of residues 3–12 and 17–26, also using the coordinates of the corresponding atoms for performing the (non-mass-weighted) least-squares fit superposition [63] of successive structures onto the reference one. The (non-mass-weighted) radius of gyration R_{gyr} was calculated along each trajectory at 10 ps intervals based on all atoms of the same residues. Intra-solute WC H—bonds were monitored along each trajectory at 10 ps intervals. A H—bond is assumed to exist between a donor atom, a hydrogen atom bound to this donor atom and an acceptor atom, if the distance between the hydrogen and the acceptor is smaller than 0.25 nm and the angle between the donor-hydrogen and hydrogen-acceptor vectors is larger than 135°. RDF corresponding to the (minimum-image) distances between all pairs of phosphorus–phosphorus atoms in the same strand (P–P), phosphorus–phosphorus atoms in different strands (P–P′), phosphorus–sodium atoms (P–Na), and sodium–sodium atoms (Na–Na) were determined separately as an average over trajectory frames sampled at 1 ps intervals from the last 2 ns of each trajectory.

All analysis programs were implemented in Jython and Mathematica as extensions to the open-source molecular mechanics analysis package esra [64]. Visualisations were performed using the PyMol program [65].

Table 1. Summary of the five simulations performed in the present study.

Code	Box	Elec.	R_c (nm)
CL	CU	LS	–
$CR_{1.4}$	CU	TW/RF	1.4
$CR_{2.0}$	CU	TW/RF	2.0
$TR_{1.4}$	TO	TW/RF	1.4
$TR_{2.0}$	TO	TW/RF	2.0

Note: CU, cubic box of edge length 6.6 nm, containing one tetradecanucleotide dimer, 26 sodium ions and 9060 water molecules; TO, truncated octahedral box based on a cubic box of edge length 7.7 nm, containing one tetradecanucleotide dimer, 26 sodium ions and 6927 water molecules; TW/RF, twin-range/reaction-field method with a long-range cutoff radius R_c (together with a short-range cutoff radius of 0.8 nm, an update frequency of five timesteps for the short-range pairlist and intermediate-range interactions, and a RF dielectric permittivity of 60); LS, lattice-sum (particle–particle–particle–mesh) method.

3. Results

The RMSD values (with reference to an idealised B-DNA structure and calculated for residues 3–12 and 17–26) along each of the five trajectories (Table 1) are shown in Figure 1 as a function of time. Only the simulation employing the LS electrostatic scheme displays an essentially stable RMSD along the 10 ns trajectory (increasing only slightly from 0.4 to 0.7 nm). In contrast, all simulations employing the TW/RF scheme show a steady increase of the deviation from the initial structure, and reach final RMSD values of 1–1.2 nm after 10 ns.

The R_{gyr} values (calculated for residues 3–12 and 17–26) along each of the five trajectories (Table 1) are shown in Figure 2 as a function of time. Here also, only the simulation employing the LS electrostatic scheme displays a nearly constant R_{gyr} of about 1.25 nm. The simulations employing the TW/RF scheme with a long-range cutoff distance of 1.4 nm show a steady decrease in this quantity (reaching values of about 1.1 nm after 10 ns of simulation), indicating the formation of a more compact structure. Conversely, the simulations employing the TW/RF scheme with a long-range cutoff distance of 2 nm show a steady increase in this quantity (reaching values of about 1.6 nm after 10 ns of simulation), indicating the formation of a more extended structure.

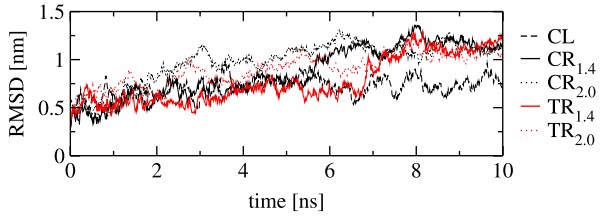

Figure 1. Time-evolution of the atom-positional RMSD from the initial (idealised) B-DNA structure, calculated based on all atoms of residues 3–12 and 17–26. See Table 1 for the simulation codes.

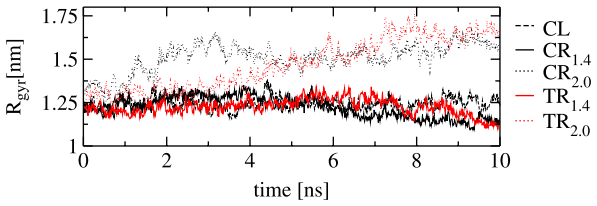

Figure 2. Time-evolution of the (non-mass-weighted) radius of gyration (R_{gyr}), calculated based on all atoms of residues 3–12 and 17–26. See Table 1 for the simulation codes.

The occurrence of WC base-pairing (complete, partial or inexistent fulfilment of the two A═T or three G≡C H—bonds between two bases in the WC scheme) along each of the trajectories (Table 1) is shown in Figure 3. In three of the five simulations ($TR_{1.4}$, $CR_{2.0}$ and $TR_{2.0}$), the WC base-pairing scheme is entirely disrupted at the end of the simulation. For simulation $CR_{2.0}$, this disruption already occurs during the first 1.5–2 ns of the simulation (simultaneously with an important increase in the RMSD and R_{gyr} values, see Figures 1 and 2). The loss of native base-pairing is more progressive (from the terminal to the central base-pairs) for simulations $TR_{1.4}$ and $TR_{2.0}$, but nevertheless

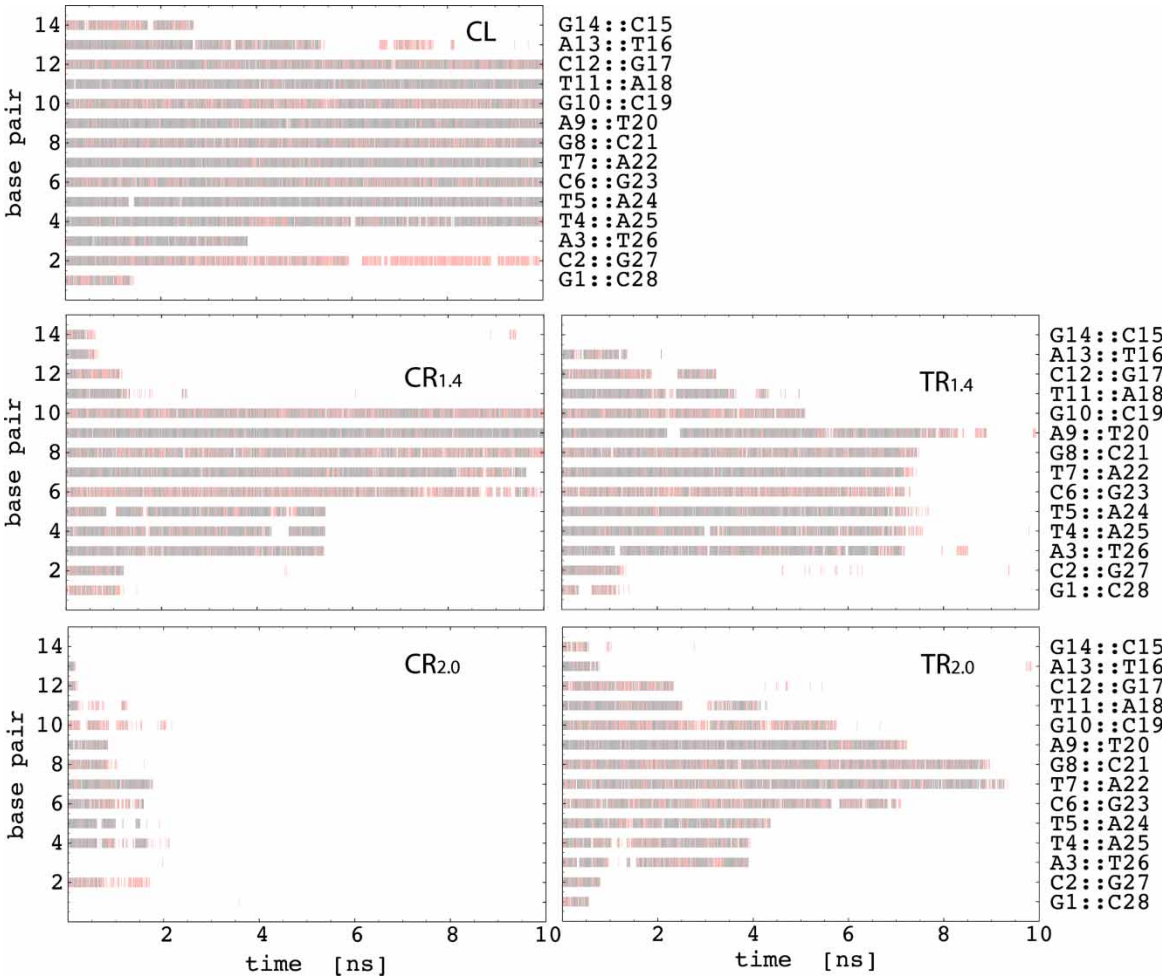

Figure 3. Time-evolution of the occurrence of WC base-pairing between corresponding base-pairs. The base-pairing may be complete (black; the two A═T or three C≡G H—bonds of the WC scheme are present simultaneously), partial (red; at least one of the H—bonds of the WC scheme is present) or inexistent (no symbol). The corresponding bases on the two strands are indicated on the right. See Table 1 for the simulation codes.

completed after 8–9 ns of simulation. In the simulation $CR_{1.4}$, all base-pairs except A9═T20 are partially (C6≡G23, G8≡C21 and G10≡C19) or entirely disrupted by the end of the simulation. In contrast, in the simulation CL employing the LS electrostatic scheme, all base-pairs except G1≡C28, C2≡G27, A3═T26, A13═T16 and G14≡C15 (terminal base-pairs) are essentially stable throughout the 10 ns trajectory. The base-pairs C2≡G27 and A13═T16 exhibit reversible disruption and reformation events throughout the simulation (alternating between complete, partial and inexistent WC base-pairing), although the general evolution is towards their disappearance. A more general H—bond analysis of the trajectory also reveals that the base-pair A3═T26 converts to a Hoogsteen-type pairing [62,66] after about 4 ns of simulation, which is then stable throughout the remainder of the trajectory. These observations clearly show that the WC base-pairing scheme is unstable (within the force-field employed) for all simulations employing the TW/RF scheme. They also suggest that this pairing scheme may be stable (except for the 2–3 terminal base-pairs at each end of the duplex) when employing the LS scheme. Although this second statement is certainly valid on the 10 ns time scale, the present simulation remains too short to assess its general validity. In particular, it cannot be ruled out that progressive disruption of WC base-pairing (starting from the termini) also occurs in the LS simulation, but takes place on a slower time scale compared to the TW/RF simulations.

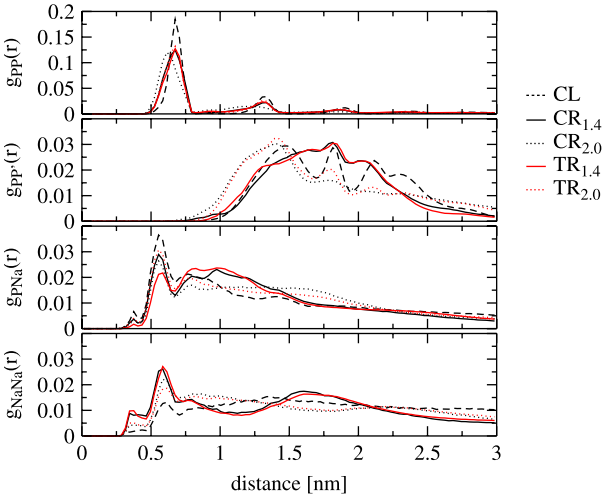

Figure 4. RDFs calculated for the last 2 ns of the different (10 ns total) simulations. From the top: phosphorus–phosphorus distances for atoms belonging to the same strand (P–P), phosphorus–phosphorus distances for atoms belonging to opposing strands (P–P′), phosphorus–sodium distances (P–Na), and sodium–sodium distances (Na–Na). Note the different scale used for the first graph. See Table 1 for the simulation codes.

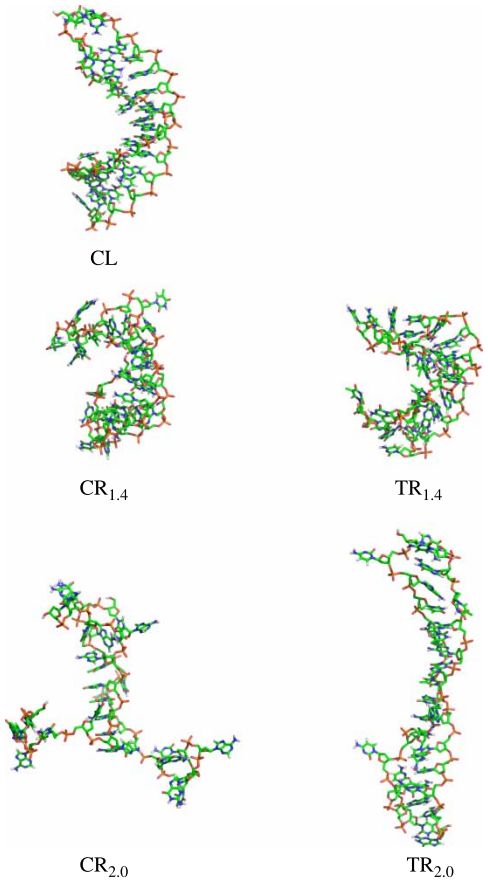

Figure 5. Final structures of the different simulations (after 10 ns). All structures are drawn at the same scale. See Table 1 for the simulation codes.

The RDFs associated with the P–P (same strand), P–P′ (different strands), P–Na and Na–Na distances, averaged over the last 2 ns of each simulation (Table 1) are shown in Figure 4. For the P–P RDF in the simulation using the LS electrostatic scheme, a sharp maximum is found at a distance of 0.7 nm, as well as successive broader peaks of progressively decreasing magnitudes at distances of 1.3, 1.9 and 2.4 nm. These peaks approximately correspond to the distances between first-, second-, third- and fourth-neighbour phosphate groups along a given strand of a canonical B-DNA duplex. Similar behavior with somewhat broadened peaks is found for all other simulations, except simulation $CR_{2.0}$. In the latter simulation, a sharp maximum is found at a distance of 0.6 nm, followed by a very broad peak centred at about 1.2 nm. For the P–P′ RDF in the simulation using the LS electrostatic scheme, sharp maxima are found at successive distances of 1.5, 1.8, 2.1 and 2.3 nm, approximately corresponding to the distances between first-, second-, third- and fourth-

neighbour phosphate groups along the opposing strands of a canonical B-DNA duplex. The two simulations employing the TW/RF electrostatic scheme with a cutoff distance of 1.4 nm exhibit one broad essentially featureless distribution centred at 1.8 nm. For the two simulations employing the TW/RF electrostatic scheme with a cutoff distance of 2 nm, the distribution is also broad and essentially featureless, but centred at a much shorter distance of 1.4 nm. For the P–Na RDFs, a sharp peak is found for all simulations at a distance of 0.6 nm, corresponding to the phosphate–sodium contact distance. A second, lower and broader peak is found at a distance of 0.8 nm, corresponding to the solvent-separated ion pair. Beyond this second peak, the CL simulation shows a gradual tapering-off, the $CR_{1.4}$ and $TR_{1.4}$ simulations show a broad third peak around 1 nm, and the $CR_{2.0}$ and $TR_{2.0}$ simulations show a broad shoulder in the region between 1 and 1.8 nm. Finally, the Na–Na RDFs present two peaks at 0.35 and 0.6 nm for all simulations, corresponding to the contact and solvent-separated ion pairs. The heights of these peaks decrease when going successively from TW/RF simulations with a cutoff distance of 1.4 nm to TW/RF simulations with a cutoff distance of 2 nm, and to the LS simulation. Beyond the second peak, the CL simulation shows a very broad peak centred at a distance of about 1.4 nm, the $CR_{1.4}$ and $TR_{1.4}$ simulations show a broad well centred at 1.2 nm followed by a broad peak centred at 1.6 nm, and the $CR_{2.0}$ and $TR_{2.0}$ simulations show a very broad well centred at 1.7 nm followed by a very broad peak centred at 2.2 nm.

Based on the four sets of RDF curves, it appears that TW/RF simulations employing the same long-range cutoff distance present very similar features irrespective of the box size and geometry, while important differences are found between simulations employing different electrostatic schemes or cutoff distances.

The above findings concerning the P–Na and Na–Na RDFs are consistent with the results of continuum electrostatics analyses for simple spherical ions [67–69] insofar as: (i) artificial periodicity in LS simulations has little influence on the potential of mean force for interaction between small ions in a high dielectric medium such as water; and (ii) cutoff truncation in RF simulations is expected to affect this potential of mean force more significantly, especially in the distance ranges just below and just above the cutoff distance. However, the above continuum electrostatics studies suggest that the RF scheme tends to stabilise like-charge ion pairs just below the cutoff distance and to destabilise them just above the cutoff distance (the converse being suggested for opposite-charge ion pairs). In contrast, in the present study (as well as in previous explicit-solvent simulations of aqueous sodium chloride [70]), it is found that like-charge ion pairs (Na–Na) are destabilised just below the cutoff distance, and stabilised just above, with the converse being observed for opposite-charge ion pairs (P–Na). The reason for this discrepancy between continuum electrostatics and explicit-solvent results remains unclear at present.

The effect of the electrostatic scheme on the P–P and P–P′ RDFs is more difficult to interpret, because the relative locations of the phosphate groups are largely influenced by covalent constraints within the DNA structure (i.e. these charged cannot freely move in solution). However, the influence of the chosen electrostatic scheme or cutoff distance is obviously also very large.

The final structures of each of the five trajectories (Table 1) are shown in Figure 5. In all cases except simulation CL, the double-helical structure is entirely disrupted at the end of the simulation. These final structures (as well as all previous observations) suggest that the box size and geometry (and therefore, to some extent, the counterion concentration) have a much lower impact on the simulations than the electrostatic scheme or the cutoff distance. The CL simulation preserves a double-helical structure, in spite of a significant bending and important fraying of the terminal base-pairs. The simulations employing TW/RF electrostatics with a long-range cutoff distance of 1.4 nm lead to compact, 'globular' structures. In contrast, the simulations employing TW/RF electrostatics with a long-range cutoff distance of 2 nm, lead to rather extended structures, where cross-strand base stacking is preferred over base-pairing.

4. Conclusions

In the present study, we reported and compared five long-timescale (10 ns) explicit-solvent MD simulations of a tetradecanucleotide dimer in water using the GROMOS 45A4 force-field [49] and the SPC water model [54]. Four independent simulations employing the TW/RF scheme (with computational boxes of two different shapes and sizes, and two different values for the long-range cutoff distance) led to dramatic distortions from the canonical B-DNA initial structure and (nearly) complete loss of WC base-pairing. A single simulation employing the LS scheme essentially led to the preservation of the native structure on the 10 ns timescale (in spite of a significant bending) and of the WC base-pairing (except for the 2–3 terminal base-pairs at both ends of the dimer). These differences observed between the two schemes seem correlated with large differences in the RDFs between charged entities (backbone phosphate groups and sodium counterions) within the system.

In view of these results, it may be tempting to conclude that the LS method is more accurate than the RF method, and represents the appropriate scheme to be

employed in MD simulations of nucleic acids. However, although the present simulations provide strong evidence in this direction, they are not rigorously sufficient to prove this statement. In particular, the following considerations should be kept in mind:

a. The tetradecanucleotide duplex might be intrinsically unstable (in which case the LS result would be incorrect). However, experimental evidence suggests that this is not the case [51].
b. The tetradecanucleotide duplex might be unstable within the force-field employed, when assuming a hypothetically exact treatment of electrostatic interactions (in which case the LS result could be caused by an artificial stabilisation of the native state or a large decrease of the denaturation rate, e.g. caused by periodicity artefacts).
c. Individual MD trajectories have in principle little significance, unless they can cover the entire extent of configurational space accessible to the system (on the 'experimental' time scale). This requirement is not fulfilled in the present case and the choice of arbitrary initial conditions may bias observations made on the individual trajectories. Thus, it could be argued that the duplex denaturation observed in a TW/RF simulation is caused by an unfavorable choice of initial conditions (unlucky trajectory) and the stability observed in the LS simulation by a favorable choice (lucky trajectory). However, not only do the simulations using TW/RF systematically show an almost complete denaturation, but they also afford similar end states for simulations using the same cutoff distance. This reduces the likelihood of the former suggestion.
d. If the tetradecanucleotide duplex is stable within the force field employed when assuming a hypothetically exact treatment of electrostatic interactions, and omitting the considerations of point c, the stability of the native state in LS simulations is not yet a definitive proof for the accuracy of this scheme. There are many ways to achieve the stability of a structure through a physically incorrect model (e.g. by application of position restrains). On the other hand, the denaturation observed in the TW/RF simulations would then be sufficient to prove the inaccuracy of this scheme.

We believe that the (possibly) most convincing objection is that of point b, because: (i) artificial periodicity in LS simulations has been suggested to generally stabilise the native (i.e. usually one of the most compact) structure of biomolecules [21]; and (ii) the TW/RF scheme (in contrast to the LS scheme) as used in this study (truncation based on distances between charge-groups) is affected by important algorithmic noise (cutoff noise), which might cause equipartition violations as well as accelerate the spontaneous evolution of the system. In other words, if the B-DNA form is intrinsically unstable within the present force field, it may be that the LS method artificially stabilises the native state and slows down the denaturation (to the extent that it no longer occurs on the 10 ns timescale, if at all).

Keeping these possible objections in mind, the results of the present study nevertheless suggest that, in the current state of knowledge, the LS scheme should probably be preferred over the TW/RF scheme for performing explicit-solvent simulations of nucleic acids.

Acknowledgements

Financial support from the Swiss National Foundation, grant No. 200020-109261/1 is gratefully acknowledged.

References

[1] T.E. Cheatham and P.A. Kollman, *Molecular dynamics simulation of nucleic acids*, Annu. Rev. Phys. Chem. 51 (2000), pp. 435–471.
[2] T.E. Cheatham and M.A. Young, *Molecular dynamics simulation of nucleic acids: successes, limitations, and promise*, Biopolymers 56 (2001), pp. 232–256.
[3] E. Giudice and R. Lavery, *Simulations of nucleic acids and their complexes*, Acc. Chem. Res. 35 (2002), pp. 350–357.
[4] J. Norberg and L. Nilsson, *Molecular dynamics applied to nucleic acids*, Acc. Chem. Res. 35 (2002), pp. 465–472.
[5] T.E. Cheatham, *Simulation and modeling of nucleic acid structure, dynamics and interactions*, Curr. Opin. Struct. Biol. 14 (2004), pp. 360–367.
[6] D.E. Draper, D. Grilley, and A.M. Soto, *Ions and RNA folding*, Annu. Rev. Biophys. Biomol. Struct. 34 (2005), pp. 221–243.
[7] Y. Cheng, N. Korolev, and L. Nordenskio, *Similarities and differences in interaction of K^+ and Na^+ with condensed ordered DNA. A molecular dynamics computer simulation study*, Nucl. Acids Res. 34 (2006), pp. 686–696.
[8] M.A. Kastenholz, I.U. Schwartz, and P.H. Hünenberger, *Investigation of the transition between the B and Z conformations of DNA by targeted molecular dynamics simulations with explicit solvation*, Biophys. J. 91 (2006), pp. 2976–2990.
[9] T.E. Cheatham and B.R. Brooks, *Recent advances in molecular dynamics simulation towards the realistic representation of biomolecules in solution*, Theoret. Chem. Acc. 99 (1998), pp. 279–288.
[10] P.P. Ewald, *Die Berechnung optischer und elektrostatischer Gitterpotentiale*, Ann. Phys. 64 (1921), pp. 253–287.
[11] R.W. Hockney and J.W. Eastwood, *Computer Simulation Using Particles*, 2nd ed., Institute of Physics Publishing, Bristol, 1988.
[12] P.H. Hünenberger, *Lattice-sum methods for computing electrostatic interactions in molecular simulations*, in *Simulation and Theory of Electrostatic Interactions in Solution: Computational Chemistry, Biophysics, and Aqueous Solution*, G. Hummer and L.R. Pratt, eds., American Institute of Physics, New York, 1999.
[13] T. Darden, D. York, and L. Pedersen, *Particle mesh Ewald: An N log(N) method for Ewald sums in large systems*, J. Chem. Phys. 98 (1993), pp. 10089–10092.
[14] U. Essmann et al., *A smooth particle mesh Ewald method*, J. Chem. Phys. 103 (1995), pp. 8577–8593.
[15] T.N. Heinz and P.H. Hünenberger, *Combining the lattice-sum and reaction-field approaches for computing electrostatic interactions in molecular simulations*, J. Chem. Phys. 123 (2005), pp. 034107/1–034107/19.

[16] M. Kastenholz and P.H. Hünenberger, *Development of a lattice-sum method emulating nonperiodic boundary conditions for the treatment of electrostatic interactions in molecular simulations: a continuum electrostatics study*, J. Chem. Phys. 124 (2006), pp. 124108/1–124108/12.

[17] B.A. Luty and W.F. van Gunsteren, *Calculating electrostatic interactions using the particle–particle particle–mesh method with nonperiodic long-range interactions*, J. Phys. Chem. 100 (1996), pp. 2581–2587.

[18] P.E. Smith and B.M. Pettitt, *Ewald artifacts in liquid state molecular dynamics simulations*, J. Chem. Phys. 105 (1996), pp. 4289–4293.

[19] P.E. Smith, H.D. Blatt, and B.M. Pettitt, *On the presence of rotational ewald artifacts in the equilibrium and dynamical properties of a zwitterionic tetrapeptide in aqueous solution*, J. Phys. Chem. B 101 (1997), pp. 3886–3890.

[20] P.H. Hünenberger and J. Andrew McCammon, *Ewald artifacts in computer simulations of ionic solvation and ion–ion interaction: a continuum electrostatics study*, J. Chem. Phys. 110 (1999), pp. 1856–1872.

[21] ———, *Effect of artificial periodicity in simulations of biomolecules under Ewald boundary conditions: a continuum electrostatics study*, Biophys. Chem. 78 (1999), pp. 69–88.

[22] W. Weber, P.H. Hünenberger, and J.A. McCammon, *Molecular dynamics simulations of a polyalanine octapeptide under Ewald boundary conditions: influence of artificial periodicity on peptide conformation*, J. Phys. Chem. B 104 (2000), pp. 3668–3675.

[23] S. Boresch and O. Steinhauser, *The dielectric self-consistent field method. I. Highways, byways, and illustrative results*, J. Chem. Phys. 115 (2001), pp. 10780–10792.

[24] ———, *The dielectric self-consistent field method. II. Application to the study of finite range effects*, J. Chem. Phys. 115 (2001), pp. 10793–10807.

[25] P. Mark and L. Nilsson, *Structure and dynamics of liquid water with different long-range interaction truncation and temperature control methods in molecular dynamics simulations*, J. Comput. Chem. 23 (2002), pp. 1211–1219.

[26] M.A. Kastenholz and P.H. Hünenberger, *Influence of artificial periodicity and ionic strength in molecular dynamics simulations of charged biomolecules employing lattice-sum methods*, J. Phys. Chem. B 108 (2004), pp. 774–788.

[27] I. Chandrasekhar et al., *Molecular dynamics simulation of lipid bilayers with GROMOS96: application of surface tension*, Mol. Simul. 31 (2005), pp. 543–548.

[28] M.A. Villarreal and G.G. Montich, *On the Ewald artifacts in computer simulations. The test-case of the octaalanine peptide with charged termini*, J. Biomol. Struct. Dyn. 23 (2005), pp. 135–142.

[29] M.A. Kastenholz and P.H. Hünenberger, *Computation of methodology-independent ionic solvation free energies from molecular simulations. I. The electrostatic potential in molecular liquids*, J. Chem. Phys. 124 (2006), p. 123106.

[30] ———, *Computation of methodology-independent ionic solvation free energies from molecular simulations. II. The hydration free energy of the sodium cation*, J. Chem. Phys. 124 (2006), p. 1.

[31] J.A. Barker and R.O. Watts, *Monte Carlo studies of the dielectric properties of water-like models*, Mol. Phys. 26 (1973), pp. 789–792.

[32] J.A. Barker, *Reaction field, screening, and long-range interactions in simulations of ionic and dipolar systems*, Mol. Phys. 83 (1994), pp. 1057–1064.

[33] P.H. Hünenberger and W.F. van Gunsteren, *Alternative schemes for the inclusion of a reaction-field correction into molecuar dynamics simulations: influence on the simulated energetic, structural, and dielectric properties of liquid water*, J. Chem. Phys. 108 (1998), pp. 6117–6134.

[34] I.G. Tironi et al., *A generalized reaction field method for molecular dynamics simulations*, J. Chem. Phys. 102 (1995), pp. 5451–5459.

[35] W.F. van Gunsteren et al., *Biomolecular Simulation: The GROMOS96 Manual and User Guide*. Verlag der Fachvereine, Zürich, 1996.

[36] T.E. Cheatham et al., *Molecular-dynamics simulations on solvated biomolecular systems – the particle mesh Ewald method leads to stable trajectories of DNA, RNA, and proteins*, J. Am. Chem. Soc. 117 (1995), pp. 4193–4194.

[37] J. Norberg and L. Nilsson, *On the truncation of long-range electrostatic interactions in DNA*, Biophys. J. 79 (2000), pp. 1537–1553.

[38] S. Swaminathan, G. Ravishanker and D.L. Beveridge, *Molecular dynamics of B-DNA including water and counterions: a 140-ps trajectory for d(CGCGAATTCGCG) based on the GROMOS force field*, J. Am. Chem. Soc. 113 (1991), pp. 5027–5040.

[39] A.M.J.J. Bonvin et al., *Water molecules in DNA recognition II: A molecular dynamics view of the structure and hydration of the trp operator*, J. Mol. Biol. 282 (1998), pp. 859–873.

[40] M. Nina and T. Simonson, *Molecular dynamics of the tRNA^{Ala} acceptor stem: comparison between continuum reaction field and particle–mesh Ewald electrostatic treatments*, J. Phys. Chem. B 106(14) (2002), pp. 3696–3705.

[41] T. Soares et al., *Alpha- and beta-polypeptides show a different stability of helical secondary structure*, Tetrahedron 60 (2004), pp. 7775–7780.

[42] J. Dolenc et al., *Molecular dynamics simulations and free energy calculations of netropsin and distamycin binding to an AAAAA DNA binding site*, Nucl. Acids Res. 33 (2005), pp. 725–733.

[43] U. Dornberger, M. Leijon and H. Fritzsche, *High base pair opening rates in tracts of GC base pairs*, J. Biol. Chem. 274 (1999), pp. 6957–6962.

[44] P.K. Bhattacharya, J. Cha and J.K. Barton, *^{1}H-NMR determination of base-pair lifetimes in oligonucleotides containing single base mismatches*, Nucl. Acids Res. 30 (2002), pp. 4740–4750.

[45] P.J. Steinbach and B.R. Brooks, *New spherical-cutoff methods for long-range forces in macromolecular simulation*, J. Comput. Chem. 15 (1994), pp. 667–683.

[46] C.L. Brooks, III, B.M. Pettitt and M. Karplus, *Structural and energetic effect of truncating the long ranged interactions in ionic and polar fluids*, J. Chem. Phys. 83 (1985), pp. 5897–5908.

[47] K.J. McConnell et al., *A nanosecond molecular dynamics trajectory for a B DNA double helix: evidence for substates*, J. Am. Chem. Soc. 116 (1994), pp. 4461–4462.

[48] A.D. MacKerell, *Influence of magnesium ions on duplex DNA structural, dynamic, and solvation properties*, J. Phys. Chem. B 101 (1997), pp. 646–650.

[49] T.A. Soares et al., *An improved nucleic-acid parameter set for the GROMOS force field*, J. Comput. Chem. 26 (2005), pp. 725–737.

[50] R.D. Lins and P.H. Hünenberger, *A new GROMOS force field for hexopyranose-based cardohydrates*, J. Comput. Chem. 26 (2005), pp. 1400–1412.

[51] B. Heddi et al., *Quantification of DNA BI/BII backbone sub-states in solution. Implications for DNA overall structure and recognition*, J. Am. Chem. Soc. 128 (2006), pp. 9170–9177.

[52] W.R.P. Scott et al., *The GROMOS biomolecular simulation program package*, J. Phys. Chem. A 103 (1999), pp. 3596–3607.

[53] M. Christen et al., *The GROMOS software for biomolecular simulation: GROMOS05*, J. Comput. Chem. 26 (2005), pp. 1719–1751.

[54] H.J.C. Berendsen et al., *Interaction models for water in relation to protein hydration*, in *Intermolecular Forces*, B. Pullman ed., Reidel, Dordrecht, 1981, pp. 331–342.

[55] M. Dixon and S. Reich, *Symplectic time-stepping for particle methods*, GAMM Mitteilungen 27 (2004), pp. 9–24.

[56] J-P. Ryckaert, G. Ciccotti and H.J.C. Berendsen, *Numerical integration of the cartesian equations of motion of a system with constraints: molecular dynamics of n-alkanes*, J. Comput. Phys. 23 (1977), pp. 327–341.

[57] H.J.C. Berendsen et al., *Molecular dynamics with coupling to an external bath*, J. Chem. Phys. 81 (1984), pp. 3684–3690.

[58] T.N. Heinz, W.F. van Gunsteren and P.H. Hünenberger, *Comparison of four methods to compute the dielectric permittivity of liquids from molecular dynamics simulations*, J. Chem. Phys. 115 (2001), pp. 1125–1136.

[59] P.H. Hünenberger, *Optimal charge-shaping functions for the particle–particle–particle–mesh (P^3M) method for computing*

electrostatic interactions in molecular simulations, J. Chem. Phys. 113 (2000), pp. 10464–10476.

[60] D.L. Beveridge et al., *Molecular dynamics simulations of the 136 unique tetranucleotide sequences of DNA oligonucleotides. I. Research design and results on d(cpg) steps*, Biophys. J. 87 (2004), pp. 3799–3813.

[61] S.B. Dixit et al., *Molecular dynamics simulations of the 136 unique tetranucleotide sequences of DNA oligonucleotides. II. Sequence context effects on the dynamical structures of the 10 unique dinucleotide steps*, Biophys. J. 89 (2005), pp. 3721–3740.

[62] W. Saenger, *Principles of Nucleic Acid Structure*, Springer, New York, 1984.

[63] S.K. Kearsley, *On the orthogonal transformation used for structural comparisons*, Acta Cryst. A 45 (1989), pp. 208–210.

[64] V. Kräutler, M. Kastenholz and P.H. Hünenberger, *The esra molecular mechanics analysis package*, available at http://esra.sf.net/ (2005).

[65] W.L. DeLano, *The PyMOL molecular graphics system*, available at http://www.pymol.org (2002).

[66] K. Hoogsteen, *The crystal and molecular structure of a hydrogen-bonded complex between 1-methylthymine and 9-methyladenine*, Acta Cryst. 16 (1963), pp. 907–916.

[67] C. Peter, P.H. Hünenberger and W.F. van Gunsteren, *Solving the Poisson equation for solute–solvent systems using fast Fourier transforms*, J. Chem. Phys. 116 (2002), pp. 7434–7451.

[68] M. Bergdorf, C. Peter and P.H. Hünenberger, *Influence of cutoff truncation and artificial periodicity of electrostatic interactions in molecular simulations of solvated ions: a continuum electrostatics study*, J. Chem. Phys. 119 (2003), pp. 9129–9144.

[69] C.P.H. Peter, W.F. van Gunsteren and P.H. Hünenberger, *A fast-Fourier-transform method to solve continuum-electrostatics problems with truncated electrostatic interactions: algorithm and application to ionic solvation and ion–ion interaction*, J. Chem. Phys. 119 (2003), pp. 12205–12223.

[70] D. Trzesniak, *Personal communication*, 2006.